YAEC 1571

HAZARDS ANALYSES OF SEABROOK STATION

CHARCOAL FILTER UNITS

Seabrook Station
Public Service Company of New Hampshire
New Hampshire Yankee Division

Revision 1

November 1991

Prepared by David M. Pepe — 10-3-86 Date

Reviewed by Alexander R. Klein — 10-8-86 Date

Approved by William J. Cloutier — 10/9/86 Date

REVISION 1		
PREPARED BY\DATE	REVIEWED BY\DATE	APPROVED BY\DATE
11-21-91	11/22/91	11-22-91

Yankee Atomic Electric Company
Nuclear Services Division
1671 Worcester Road
Framingham, Massachusetts 01701

DISCLAIMER OF RESPONSIBILITY

This document was prepared by Yankee Atomic Electric Company ("Yankee"). The use of information contained in this document by anyone other than Yankee, or the Organization for which the document was prepared, is not authorized and with respect to any unauthorized use, neither Yankee nor its officers, directors, agents, or employees assume any obligation, responsibility, or liability or makes any warranty or representation of the material contained in the document.

TABLE OF CONTENTS

SUBJECT	PAGE
Introduction	1
Background	1
Discussion	1-6
Conclusion	6
Evaluation of Charcoal Filer Unit Fires at Seabrook Station - PLC	Appendix I
Iodine Adsorber Fire Test - Nuclear Consulting Services, Inc.	Appendix II

INTRODUCTION

This report describes a Hazards Analysis conducted on Seabrook Station's filter units, which contain charcoal beds/cells. Table 1 identifies Seabrook's nine (9) filter units and their location.

BACKGROUND

Seabrook's approach to a charcoal fire within the filter units is fire prevention and detection as outlined within the guidelines of Item II.B(3) of 10CFR50, Appendix R, which states, "specify measures for fire prevention, fire detection, fire suppression, and fire containment, and alternative shutdown capability as required for each fire area containing structures, systems, and components important to safety in accordance with NRC guidelines and regulations."

To address internal charcoal fires, an analysis was conducted on all Seabrook filter units, which contain charcoal beds/cells, to determine the maximum temperatures of the charcoal adsorber sections, due to decay heat from iodine and its daughter product decay without air flow. This analysis showed that the overall maximum temperature would be limited to 170°F. Additional analyses indicate that the maximum temperature for the HEPA filters (due to decay heat from the particulate iodines accumulated in these filters) will be limited to 187°F. These temperatures are well below the maximum limit of 300°F recommended in ANSI-N509-1980. Thus, there is no possibility of an internal charcoal fire due to decay heat.

Seabrook's charcoal adsorber filters are also protected from external fires since they are contained in a combination of heavy metal casing, wire debris screens, and fire retardant HEPA filters as recommended in Regulatory Guide 1.52, Design, Testing, and Maintenance Criteria for Post-Accident Engineered - Safety Feature Atmosphere Cleanup System Air Filtration and Adsorption Units of Light-Water-Cooled Nuclear Power Plants, Revision 2, March 1978.

Further, transient combustibles are limited administratively. Any welding or open flame sources will be controlled and limited. A fire watch will be maintained per plant administrative procedures during these activities. These precautions will prevent external sources from causing internal combustion to the charcoal beds/cells.

However, a fire hazard analysis is developed in this report to address the effects of a postulated charcoal fire in the filter units and its impact on equipment needed for safe shutdown. A realistic, but conservative approach was used to model the charcoal fires since charcoal is a slow burning medium.

DISCUSSION

The following assumptions were used in this hazard analysis.

1. Fire will be detected by reliable and early warning system.

2. From detection, which is alarmed in Control Room, Operations per Operating Procedures will shutdown air flow to the filter units. Assume five minutes time from alarm conditions to shutdown of air flow. Charcoal is assumed to be ignited in this time frame.

3. The Fire Brigade will respond to the charcoal filter within 20 minutes from notification by the Control Room for all protected plant areas except Containment. This notification is per Operating Procedures. For a fire within Containment, the Fire Brigade will respond within 90 minutes. (See Engineering Evaluation EE-05-033, Revision 00.)

4. Ignition of the charcoal starts at the top of the charcoal bed/cell. This is assumed conservative since a fire located lower in the bed/cell would burn the retaining mesh and drop the charcoal from the air flow path precluding rapid fire propagation.

5. Since a fire cannot be started due to internal decay heat, the fire must be started from an external source. Assume an outside source is carried into the filter unit. All the units have HEPA filters on the inlet before the charcoal bed. Each HEPA filter section assembly is made up of a grouping of HEPA filter elements 24" x 24" x 11-1/2". Each element is a throwaway, extended medium, dry-type filter, which are open face, rectangular, fire-resistance type design for radioactive service. Assume the source carried internal by air flow totally ignites one HEPA filter element, 2' x 2'. This 2' x 2' filter element is assumed to ignite a 4 $ft.^2$ area of the charcoal bed/cell.

6. Air flow through the charcoal bed/cell is assumed to be from the start of ignition. 4 $ft.^2$ area of charcoal will burn under air flow condition for a period of 5 minutes time. At this point forced air flow has stopped and the resulting fire will be analyzed under natural draft air flow.

7. Air flow velocity through the charcoal during forced ventilation is 40 feet per minute which is Seabrook's charcoal bed/cell design velocity.

8. Further assumptions are used in Appendix I, "Evaluation of Charcoal Filter Unit Fires at Seabrook Station," 9-29-86 by Professional Loss Control, Inc. and are noted in that Appendix.

The Hazard Analysis consist of 3 parts, (1) Determination of charcoal bed burning rates, (2) a heat transfer model of the charcoal beds/cells and (3) effects of the heat transfer on safe shutdown equipment.

(1) <u>Determination of Charcoal Bed Burning Rates</u>

A charcoal fire test was conducted by NUCON in their ASTM D3466 Test Rig. Data from this test was used by Professional Loss Control, Inc. (PLC) in their unsteady state heat transfer model of each of Seabrook's filter units, which contain charcoal beds/cells, excluding CBA-F-38 and CBA-F-8038. Each Seabrook filter was reviewed separately. NUCON's ASTM D3466 Test conducted for Seabrook used the same type of charcoal used in Seabrook's charcoal beds/cells. The test normally is performed at 100 feet per minute air velocity, however, 40 FPM velocity was used which is Seabrook's filter design velocity. The bed depth is normally 1.0 inch deep.

For Seabrook's test a 2.0 inches deep bed was used which is the limit of the ASTM D3466 apparatus. Seabrook's bed depth is 4.0 inches. Use of the test data by PLC is conservative since the test was conducted under forced air flow over a one hour period. Seabrook's filter unit heat transfer model assumes five minutes time from charcoal ignition to shutdown of air flow; where-as air flow will be shutdown five minutes after detection of a potential fire, which most likely occurs before sufficient temperature is available to ignite the charcoal.

A fire wind tunnel (FWT) test was conducted by NUCON on a 24 inch x 24 inch face area carbon adsorber specimen. The depth of the bed tested was 4.0 inches. Again, the charcoal used was the same type used at Seabrook, 2% KI and 2% TEDA impregated carbon.

The charcoal was ignited by preheating inlet air to the charcoal specimen. The specimen started burning approximately 6 minutes after CO production levels of 50 ppm were measured. Air flow was then continued for an additional 5 minutes, then stopped. Inlet and outlet temperatures were then monitored for one hour. Seabrook's anticipated alarm setpoint for CO is 50 ppm and the normal background level is 2 ppm.

The purpose of the FWT test was to look at the actual test size modeled by PLC under fire conditions.

Air flow conditions under forced ventilation were the same for the FWT test versus Seabrook's filter unit design velocity. Once the ventilation was stopped and natural drafting began, the FWT test was no longer similar to Seabrook because of duct configuration differences. Seabrook's filter units have outlet dampers, long HVAC duct runs, and in some cases inlet dampers which are isolated once the filter fans are shutdown. Thus, natural drafting through Seabrook's filters would be small. The FWT test with natural drafting indicates the charcoal fire will contain itself to a limited fire with decreasing temperature after stopping forced ventilation.

Results of the FWT test show, under conditions used in the PLC model, carbon loss for a test duration of one hour was 4.53 lbs which is approximately 10% of the test dry carbon weight. Also that CO levels increase well above normal environment levels long before a fire starts.

(2) Heat Transfer Model

The PLC unsteady heat conduction analysis looked at each charcoal filter unit, except CBA-F-38 and CBA-F-8038, to determine the net heat transfer to the filter housing surface based on charcoal temperature data supplied by NUCON. Radiation and convection heat transfer was also considered in PLC's analysis.

Radiation Heat Transfer from the fire was considered, taking into account the geometry of each of the filter units. The HEPA filters have a nominal 24" x 24" outside dimensions with a 22" x 22" steel mounting frame opening, which limits the burning material to one HEPA filter size. The burning charcoal surface area was conservatively assumed to be a 24-inch square. The larger burning surface area accounts for any fire propagation under the five minute forced ventilation period. The temperatures used in the analysis were measured within the charcoal bed on the outlet side. The highest of any of the temperatures measured was also used. Radiation Heat Loss from the steel housing to its surroundings was also considered.

For convective heat transfer, forced convection within the filter housing was neglected. If accounted for, the forced air stream would be heated and enhance the heat removal from the housing. Therefore, this assumption is conservative. Free convection heat transfer was considered on the outside of the filter housing.

Attachment II gives the detailed methodology and results of the analysis.

The following conclusions are drawn from a fire involving the charcoal beds/cells in the filter units.

1. The worst case maximum localized steel plate housing temperature was calculated to be 704°F. This temperature is substantially below that required for structural failure of the steel housing.

2. Structural failure of any steel beam or column in the vicinity of these filter units cannot be caused by heat transfer from the filter housing.

3. The maximum radiant heat emissive flux from the housing at 704°F, calculated to be less than 10 KW/m^2, is less than half the critical radiant flux necessary to ignite the worst case cable jacket materials as determined by EPRI sponsored tests at Factory Mutual Research Corporation (EPRI NP-1200, Part 1).

(3) Safe Shutdown Equipment Review

From the conclusions of the heat transfer model there would be no structural steel failures in the vicinity of Seabrook's charcoal filters. Thus no safe shutdown equipment would be effected due to steel failures. Equipment further than three feet from the filter units also would not be effected based on the maximum heat flux from the housing.

An evaluation of safe shutdown equipment was conducted looking at the equipment within and including three feet from each of the filter units.

CBA-F-38, 8038 - No charcoal fire modeling was done on these filters. It is assumed that a charcoal fire will cause loss of all equipment within its fire area (i.e., CB-F-3B-A). Seabrook's present Appendix R Safe Shutdown Study shows this to be acceptable. Also there is no concern of damage to structural steel since all this steel in this fire area is fire proofed.

CAP-F-40 - There is no safe shutdown equipment used during a fire in this fire area, PAB-F-3A-Z, within and including three feet of CAP-F-40.

CAH-F-40 - There is no safe shutdown equipment used during a fire in this fire area, C-F-3-Z, within and including three feet of CAH-F-40.

EAH-F-9, 69 - There is no safe shutdown equipment used during a fire in this fire area, CE-F-1-Z, within and including three feet of EAH-F-9,69.

FAH-F-41, 74 - There is no safe shutdown equipment used during a fire in this fire area, FSB-F1-A.

PAH-F-16 - There is no safe shutdown equipment used during a fire in this fire area PAH-F-4-Z, within and including three feet of PAH-F-16.

CONCLUSION

The hazards posed by the heating of the steel housing from a charcoal bed/cell filter fire, under the operational guidelines to shutdown forced ventilation of the filter in question, will not jeopardize the safe shutdown of Seabrook Station.

TABLE 1

Filter ID	Safety/Non	Meets RG 1.52	Area Detection	Fire Area
EAH-F-9	Safety	Yes	Yes	CE-F-1-Z Containment Enclosure EL 21' 6"
EAH-F-69	Safety	Yes	Yes	CE-F-1-Z Containment Enclosure EL 21' 6"
FAH-F-41	Safety	Yes	Yes	FSB-F1-A Fuel Building EL 84' 0"
FAH-F-74	Safety	Yes	Yes	FSB-F1-A Fuel Building EL 84' 0"
CAH-F-8	Non	No	Yes	C-F-3-Z Containment
PAH-F-16	Non	No	Yes	PAB-F-4-Z Primary Auxiliary Building EL 81' 0"
CAP-F-40	Non	No	Yes	PAB-F-3A-Z Primary Auxiliary Building EL 53' 0"
CBA-F-38	Safety	Yes	Yes	CB-F-3B-A Control Room HVAC Equipment Room EL 75'
CBA-F-8038	Safety	Yes	Yes	CB-F-3B-A Control Room HVAC Equipment Room EL 75'

PROFESSIONAL LOSS CONTROL, INC.

Attachment I to
Hazards Analyses of
Seabrook Station
Charcoal Filter Units,
YAEC 1571

Evaluation of Charcoal Filter Unit
Fires at Seabrook Station

September 29, 1986

Prepared by: James A. Milke, P.E.

Reviewed by: Michael E. Mowrer, P.E.

Approved by: Kenneth W. Dungan, P.E.

P. O. Box 446 • Oak Ridge, Tennessee 37831 • (615) 482-3541

Table of Contents

Subject	Page
Introduction	1
Background	1
Discussion	5
Conclusions	11
Analysis Methodology	Appendix A
Combustion of Wood Charcoal	Appendix B

INTRODUCTION

This report describes an engineering analysis conducted to characterize the hazard of a fire involving the charcoal filter units at the Seabrook station. An unsteady-state heat conduction analysis has been performed to predict the local temperature rise in the plate steel housing exposed to a charcoal filter fire for each of seven air handling units.

BACKGROUND

Charcoal filter beds are installed in the seven (7) air handling units identified in Table 1. Inside the housing are numerous charcoal filter bed cells. The number of cells within a housing enclosure ranges from 4 to 28. The charcoal ignition source is assumed to be external to the unit. The configuration of air cleaning systems is such that the charcoal absorbers are preceded by HEPA filters. The HEPA filter mounting frame is a steel structure with 22 inch x 22 inch openings. Therefore, no larger burning material than one HEPA filter size could enter the carbon bed. Anything larger would be stopped by the HEPA mounting frame structure even if it would penetrate the preceding components. This was the reason for the selection of a 24 inch x 24 inch exposure to a single carbon cell for both the FST test and subsequent engineering analysis.

An unsteady-state heat conduction analysis was performed on the steel housing. Since the heat conduction within the steel plate occurs very rapidly, a lumped heat capacity approach could be applied to simplify the mathematics involved. The steel housing was considered to receive radiant heat from the burning charcoal bed. Radiative and convective heat losses from the steel housing to the surroundings were included. A detailed description and the equations for the analysis are included in Appendix A.

TABLE 1

DIMENSIONS OF CHARCOAL SECTION OF UNITS

Unit	A	B	C
PAH-F-16	5'1"	12'2"	26'7"
EAH-F-9 EAH-F-69	5'1"	5'6"	3'6"
FAH-F-41 FAH-F-74	5'1"	10'3"	14'8"
CAP-F-40	5'1"	10'0"	9'11"
CAH-F-8	2'6"	5'4"	8'0"

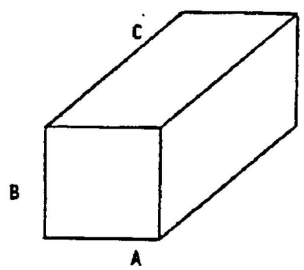

TABLE 2

(Table 1 from September 15, 1986, "Iodine Adsorber Fire Test" by Nuclear Consulting Services, Inc.)

08P3942

Test Date
3 Sept 1986

Carbon ignition followed by residual heating (i.e. air flow continued but heat off).

Method: ASTM D3466 except: 40 FPM, 2 inch bed depth and fast heat up

Material: Dry air and NUSORB KITEG II Lot 45/10

Starting condition: 25°C

Ignition occurred at an upper bed (outlet) temperature of approximately 400°C, lower bed (inlet) temperature of 285°C, air inlet temp. 285°C.

Temperatures after ignition:

Time (Min.)	Within Carbon Bed Outlet Side (°C)	Inlet Side (°C)
0:15	790	255
1:00	700	920
2:00	650	850
3:00	640	800
4:00	730	800
5:00	760	805
6:00	790	790
7:00	835	780
8:00	860	790
9:00	920	790
10:00	950	780
11:00	980	730
12:00	1050	800 purple smoke
15:00	780	450
20:00	375	250
30:00	210	150
60:00	100	135

FIGURE 1

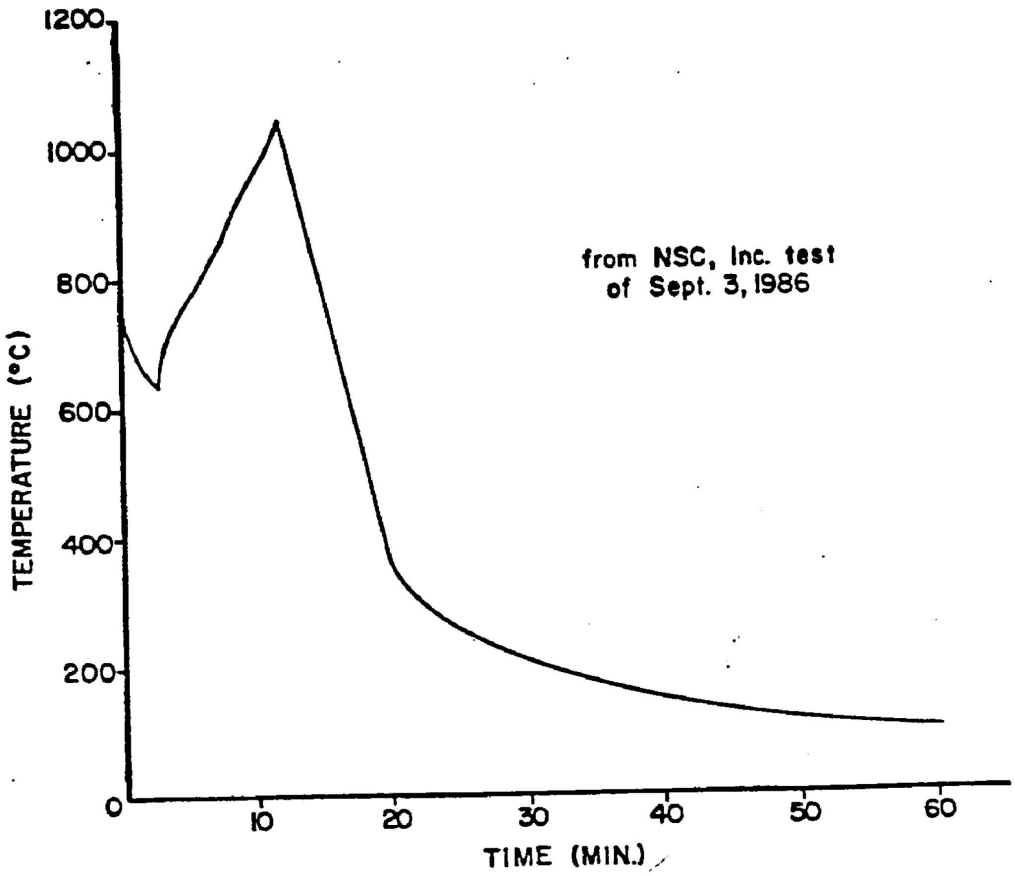

Temperature History in Charcoal Bed

DISCUSSION

The temperature rise of the steel housing on the seven charcoal filter units of concern is presented in Tables 3 through 7. As noted in the tables, the maximum localized housing temperature for Units PAH-F-16 (see Table 3), CAP-F-40 (see Table 5), FAH-F-41 and FAH-F-74 (see Table 6), are within 50°F of one another (between 411 and 461°F). The surface temperatures present a minimal hazard to fixed equipment or cabling unless mounted directly on the housing, as well as to personnel, unless they came into contact with the enclosure itself.

The maximum localized temperature predicted for Units EAH-F-9 and EAH-F-69 is 704°F (see Table 4). The increased temperature is due to the reduced size of the housing, which includes less steel through which the heat can be diffused. Still, this temperature would not appear to be at a level or exist for a sufficiently long duration to pose a serious exposure condition, unless the materials of concern are in direct contact with the housing.

Finally, because of the different air flow arrangement, the maximum temperature to the top of the enclosure for CAH-F-8 is 638°F (see Table 7). This temperature is due to the relatively small size of the enclosure unit as well as the location of the exposed side being the top of the enclosure. Being located on the top, the convective heat losses are substantially reduced from that of a side.

As noted in the tables, the analysis was terminated at 60 minutes. Extending the duration beyond 60 minutes is not necessary since the steel temperature is declining 15 to 20 minutes into the incident with no action other than shutting down the related fan within 5 minutes of the fire initiation.

TABLE 3

LOCAL HOUSING TEMPERATURE VS. TIME IN UNIT PAH-F-16

UNIT PAH-F-16 TIME (MIN)	MAXIMUM LOCAL HOUSING TEMP. (DEG F)	UNIT PAH-F-16 TIME (MIN)	MAXIMUM LOCAL HOUSING TEMP. (DEG F)
1	94	31	351
2	104	32	342
3	115	33	334
4	128	34	326
5	142	35	318
6	159	36	309
7	178	37	301
8	199	38	293
9	223	39	285
10	249	40	277
11	278	41	270
12	310	42	262
13	337	43	255
14	359	44	248
15	376	45	241
16	390	46	234
17	399	47	227
18	406	48	221
19	409	49	214
20	411	50	208
21	410	51	202
22	408	52	197
23	404	53	191
24	400	54	186
25	394	55	181
26	388	56	176
27	381	57	171
28	374	58	167
29	366	59	163
30	359	60	158

TABLE 4

LOCAL HOUSING TEMPERATURE VS.
TIME IN UNITS EAH-F-9 and EAH-F-69

UNITS EAH-F-9, EAH-F-69 TIME (MIN)	MAXIMUM LOCAL HOUSING TEMP. (DEG F)	UNITS EAH-F-9, EAH-F-69 TIME (MIN)	MAXIMUM LOCAL HOUSING TEMP. (DEG F)
1	121	31	544
2	152	32	532
3	186	33	520
4	222	34	508
5	261	35	497
6	303	36	486
7	349	37	475
8	398	38	464
9	449	39	454
10	503	40	444
11	559	41	434
12	617	42	424
13	657	43	415
14	684	44	406
15	698	45	398
16	704	46	390
17	704	47	382
18	699	48	374
19	691	49	367
20	682	50	360
21	670	51	353
22	659	52	347
23	646	53	341
24	633	54	335
25	620	55	329
26	608	56	324
27	595	57	319
28	582	58	315
29	569	59	310
30	556	60	306

TABLE 5

LOCAL HOUSING TEMPERATURE VS.
TIME IN UNITS FAH-F-41 and FAH-F-74

UNIT FAH-F-41, FAH-F-74 TIME (MIN)	MAXIMUM LOCAL HOUSING TEMP. (DEG F)	UNIT FAH-F-41, FAH-F-74 TIME (MIN)	MAXIMUM LOCAL HOUSING TEMP. (DEG F)
1	96	31	369
2	106	32	359
3	118	33	350
4	132	34	340
5	148	35	331
6	167	36	321
7	188	37	312
8	212	38	303
9	239	39	294
10	269	40	285
11	302	41	276
12	339	42	267
13	369	43	259
14	394	44	251
15	412	45	243
16	426	46	235
17	436	47	227
18	442	48	220
19	445	49	213
20	445	50	206
21	443	51	199
22	440	52	192
23	435	53	186
24	428	54	180
25	421	55	174
26	414	56	169
27	405	57	163
28	397	58	158
29	388	59	153
30	378	60	148

TABLE 6

LOCAL HOUSING TEMPERATURE VS. TIME IN UNIT CAP-F-40

UNIT CAP-F-40 TIME (MIN)	MAXIMUM LOCAL HOUSING TEMP. (DEG F)	UNIT CAP-F-40 TIME (MIN)	MAXIMUM LOCAL HOUSING TEMP. (DEG F)
1	97	31	382
2	109	32	372
3	122	33	363
4	137	34	353
5	155	35	343
6	175	36	334
7	197	37	325
8	222	38	316
9	251	39	306
10	282	40	298
11	316	41	289
12	354	42	280
13	385	43	272
14	410	44	264
15	429	45	256
16	443	46	248
17	452	47	241
18	458	48	234
19	461	49	227
20	460	50	220
21	458	51	213
22	454	52	207
23	449	53	201
24	443	54	195
25	435	55	189
26	427	56	184
27	419	57	178
28	410	58	173
29	401	59	169
30	391	60	164

TABLE 7

LOCAL HOUSING TEMPERATURE VS.
TIME IN CAH-F-8 UNIT

UNIT CAH-F-8 TIME (MIN)	MAXIMUM LOCAL HOUSING TEMP. (DEG F)	UNIT CAH-F-8 TIME (MIN)	MAXIMUM LOCAL HOUSING TEMP. (DEG F)
1	106	31	486
2	124	32	472
3	144	33	459
4	168	34	445
5	197	35	432
6	229	36	419
7	266	37	406
8	307	38	393
9	354	39	380
10	405	40	368
11	460	41	356
12	519	42	344
13	565	43	332
14	597	44	321
15	619	45	310
16	632	46	299
17	637	47	288
18	637	48	278
19	633	49	268
20	626	50	258
21	617	51	248
22	606	52	239
23	594	53	230
24	582	54	221
25	569	55	213
26	555	56	204
27	542	57	196
28	428	58	189
29	514	59	181
30	500	60	174

CONCLUSIONS

Based upon conservative, worst case calculations, the following conclusions are drawn from a fire involving the charcoal cells in the air handling units:

1. The worst case maximum localized steel plate housing temperature was calculated to be 704°F. This temperature is substantially below that required for structural failure of the steel housing.

2. Structural failure of any steel beam or column in the vicinity of these filter units cannot be caused by heat transfer from the filter housing.

3. The maximum radiant heat emissive flux from the housing at 704°F, calculated to be less than 10 kW/m^2, is less than half the critical radiant flux necessary to ignite the worst case cable jacket materials as determined by EPRI sponsored tests at Factory Mutual Research Corporation (EPRI NP-1200 part 1).

Therefore, the hazards posed by the heating of the steel housing from a charcoal bed filter cell fire will not jeopardize the safe shutdown of the plant.

File Ref: SE-02-02-103

Section F-3 Appendix D
Hazards Analyses of Seabrook Station
Charcoal Filter Units

APPENDIX A

APPENDIX A

ANALYSIS METHODOLOGY

The unsteady heat conduction analysis used for this study is described in detail in this appendix. A lumped heat capacity approach was utilized, valid as long as the heat conduction is sufficiently fast, as compared to the rate of heat transfer to the object (the appropriateness of the lumped heat capacity approach is reviewed later in this appendix).

Figure A-1 depicts the heat transfer to the steel housing. The net heat transfer to the steel acts to increase the internal energy of the steel, resulting in a temperature rise. This can be described in equation [1] as:

$$\rho c_p V \frac{dT_s}{dt} = Q_{RF} - Q_{RL} - Q_C \qquad [1]$$

where:

Q_{RF} = Radiative heat transfer from fire (W)
Q_{RL} = Radiative heat loss from steel to surroundings (W)
Q_C = Convective heat loss from steel to surroundings (W)
T_S = Steel temperature (°C)

t = Time (sec.)
ρ = Steel density (7700 kg/m^3)
C_p = Steel specific heat (520 J/kg °C)
V = Steel volume (m^3)

It should be noted that conductive losses through the steel to the remainder of the housing have been neglected. This assumption is conservative by ignoring heat which diffuses throughout the assembly.

Figure A - 1
Heat Transfer Process

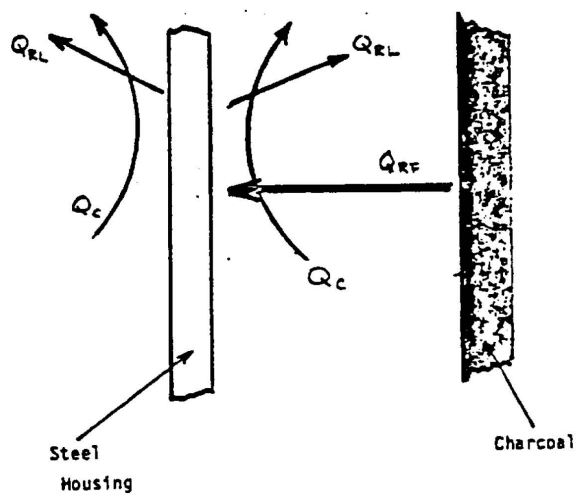

Q_c = convection heat loss
Q_{RL} = radiation heat loss
Q_{RF} = radiation from fire

The three terms involving radiation or convection heat transfer will now be described.

Radiation Heat Transfer from Fire

In general, radiation heat transfer between two finite, non-black bodies is given by:

$$Q_{RF} = \frac{\sigma (T_c^4 - T_s^4)}{\frac{1-e_c}{e_c A_c} + \frac{1}{A_c F_{cs}} + \frac{1-e_s}{e_s A_s}} \quad [2]$$

where:

σ = Stefan-Boltzmann Constant (5.67×10^{-8} W/m^2°K)
T_c = Charcoal temperature (°K)
T_s = Steel temperature (°K)
e_c = Charcoal emissivity (assume .75)
A_c = Area of burning charcoal (m^2)
F_{cs} = View factor (assume 1.0)
e_s = Steel emissivity conservatively approximated as 0.8 (1)
A_s = Area of steel (m^2)

The surface area of steel directly exposed to the radiant heat from the charcoal filter bed cell fire varied for the five distinct Unit types. For each unit, the area can be calculated as the product of dimensions "A" and "B" from Table 1, except for Unit CAH-F-8 where the area is the product of dimensions "A" and "C".

The view factor can be determined using graphs and view factor algebra. Because of the steel area being appreciably greater than the exposing charcoal bed area, the view factor was approximated as 1.0. It should be noted that since the steel and charcoal are finite in size, the view factor is actually slightly less than 1.0. Estimation of the view factor of 1.0 is conservative, i.e., this will lead to a greater steel temperature.

The charcoal emissivity is assumed to be 0.75, as suggested by Evans and Emmons (2). The burning charcoal surface area (A_C) was conservatively assumed to be 0.465 m^2 (26 inches square) which is larger than the maximum possible fire exposure (22 inches square) to the charcoal bed. The charcoal temperature is a function of time, as provided in the test report summarized in Table 2 of this report (3). The temperatures used in this analysis were measured within the charcoal bed on the outlet side. This set of temperatures was the highest of any of the temperatures measured, thereby yielding a conservative prediction of the steel temperature. This is also conservative since the temperature used is an interior temperature as opposed to a surface temperature (which the radiation is dependent on) which would be cooler.

Radiative Heat Loss

Since the temperature of the surroundings of the steel housing, other than the burning charcoal filter bed cell, is assumed to be unaffected by the fire, the surroundings will remain cool in comparison to the steel plate. As a result, radiation heat transfer will occur from the steel to the surroundings, resulting in a net heat loss from the steel. Since the surroundings are infinite in size as compared to the housing, the radiative heat loss is given by:

$$Q_{RL} = e_S A_S \sigma (T_S^4 - T_R^4) \quad [3]$$

where:

T_R = Room temperature (°K)

T_S, e_S and σ were defined previously for equation [2]. A room temperature of 27°C (81°F) was arbitrarily selected for use in the calculations.

The radiative heat loss is assumed to occur on both sides of the steel housing.

Convective Heat Loss

As long as the surrounding air temperature is less than the steel temperature, free convection heat transfer will occur. Due to the forced air flow of 40 ft/min. through the charcoal filter bed and within the housing during the first five minutes after ignition, forced convection heat transfer also can be expected. The addition of forced convection will lead to an enhanced convective heat loss from the steel. For the purpose of this analysis, the forced convection was neglected, since the forced air stream can be expected to be heated, as documented in the test report. It should be noted that the heated air temperature is expected to be less than the steel temperature. Thus, neglecting the forced convection heat transfer is conservative.

The free convection heat transfer will occur due to the heating of the air adjacent to the steel plate, resulting in air movement due to a buoyancy change. Equation [4] describes the free convection heat loss.

$$Q_c = hA_s(\Delta T) \quad [4]$$

where:

h = Convection heat transfer coefficient (W/m^2 °K)

ΔT = Temperature difference between steel and ambient air (°K).

The convection coefficient can be approximated as 4.5 W/m^2 °K (1). This value can be checked use empirically derived values for the coefficient, where the convecting fluid is air (1).

$$h = \begin{cases} 0.95\ (\Delta T)^{1/3} & \text{for vertical plate} \\ 1.43\ (\Delta T)^{1/3} & \text{for horizontal plate} \end{cases} \quad [5]$$

The condition of a horizontal plate is present for unit CAH-F-8. The value of the convection coefficient will be reviewed after the steel temperature is estimated, so that the temperature difference can be evaluated.

In the case of the units where the exposed housing surface is vertical (PAH-F-16, EAH-F-9, EAH-F-69, FAH-F-41, FAH-F-74 and CAP-F-40), the free convection heat transfer is assumed to occur on both sides of the housing. Unit CAH-F-8, with the exposed horizontal surface, the free convection is assumed to occur only from the top surface. Free convection will also exist from the lower surface, but at a much reduced rate due to the convecting air moving in opposition to smoke produced by the burning charcoal. In all cases, the ambient air temperature is arbitrarily assumed to be 27°C (81°F).

Solution for Steel Temperature

The steel temperature can be determined by substituting equations [2], [3] and [4] into equation [1]. The derivative, $\frac{dT_s}{dt}$, can be replaced by $\frac{\Delta T_s}{\Delta t}$. An iterative solution technique can be applied to determine T_s after a time duration of interest. For this study, a total time of 60 minutes was considered. In general, the equation for T_s is given as:

$$\Delta T_s = \frac{\Delta t}{\rho c_p V}\left[\frac{\sigma (T_c^4 - T_s^4)}{\frac{1-e_c}{e_c A_c} + \frac{1}{A_c} + \frac{1-e_s}{e_s A_s}} + e_s A_s \sigma (T_s^4 - T_R^4) - 4.5 A_s (T_s - T_R)\right] \quad [6]$$

Since estimates for the steel temperature are now available, the validity of two key assumptions can be checked. One assumption considered the rate of conduction heat transfer within the steel to be much greater than the radiation and convection heat transfer on the steel boundary. The second assumption stated that the convection heat transfer coefficient was 4.5 $W/m^2\ °K$. The second assumption will be addressed first, since the examination of the first assumption requires the convection coefficient to be known.

The convection heat transfer coefficient can be determined from equation [5]. Considering the temperature difference to be 200°C (an approximate

average temperature difference during the 60-minute exposure), the convection coefficient is actually 5.5 W/m^2 °K for the vertical plate and 8.43 W/m^2 °K for the horizontal plate. Thus, use of the value of 4.5 W/m^2 °K for the convection coefficient underestimated the convective heat loss, yielding greater steel temperatures. Since the assumption of 4.5 W/m^2 °K is shown to be conservative, without grossly underestimating the convective heat loss, the assumption is considered valid.

The validity of the first and more important assumption can now be assessed. The comparison of rates of conduction to convection and radiation heat transfer can be performed by evaluating the parameter, HL/k as noted in equation [7]:

$$\frac{HL}{k} < 0.1 \qquad [7]$$

where:

- H = Combined radiation and convection heat transfer coefficient (W/m^2 °K)
- L = Characteristic dimension of steel (m)
- k = Steel thermal conductivity (W/m °K)

The combined radiation and convection heat transfer coefficient is given as:

$$H = h_C + h_{RL} + h_{RF} \qquad [8]$$

where:

$$h_C = 4.5 \ W/m^2 \ °K$$

$$h_{RL} = \frac{Q_{RL}}{T_S - T_R}$$

$$h_{RF} = \frac{Q_{RF}}{T_C - T_S}$$

h_{RL} can be re-expressed as:

$$h_{RL} = \frac{Q_{RL}}{T_S - T_R} = \frac{e_S A_S \sigma (T_S^4 - T_R^4)}{T_S - T_R}$$

Similarly, h_{RF} is:

$$h_{RF} = \frac{\sigma (T_C^4 - T_S^4)}{\left(\frac{1-e_C}{e_C A_C} + \frac{1}{A_C} + \frac{1-e_S}{e_S A_S}\right)(T_C - T_S)}$$

Assuming an average steel temperature of 500 °K, average charcoal temperature of 1000 °K, and room temperature of 300 °K h_{RL} and h_{RF} can be evaluated, using the values for all other parameters which were previously presented.

h_{RL} = 56.8 W/m^{2}K

h_{RF} = 36.4 W/m^{2}K

Thus, the sum of the heat transfer coefficients is 97.7 W/m^2 °K.

The characteristic dimension of the steel (L) is the ratio of the volume to the surface area. In this case the characteristic dimension is the plate thickness, i.e., 0.001 m (1/4 inch).

Assuming the steel conductivity is estimated as 25 W/mK,

$$\frac{HL}{k} = \frac{97.7 \times .001}{25} = 0.004 < 0.1$$

Thus, the assumption of the rate of heat conduction being substantially greater than that of the convection and radiation heat transfer is appropriate.

The convective and radiative losses can also be compared to assess the sensitivity of the analysis to the selected room temperature. For illustration purposes if the assumed room temperature is increased from 81 °F to 120 °F (27 °C to 49 °C), the maximum localized housing temperature increases by only approximately 20 °F.

Selected References

1. Holman, J.P., Heat Transfer, 6th Edition, New York, McGraw Hill, 1986.

2. Evans, D.D. and Emmons, "Combustion of Wood Charcoal," Fire Research, 1, (1977), p. 57-66. (see Appendix B)

3. Nuclear Consulting Services, Inc., "Iodine Adsorber Fire Test," September 15, 1986 (unpublished).

File Ref: SE-02-02-103

Section F-3 Appendix D
Hazards Analyses of Seabrook Station
Charcoal Filter Units

APPENDIX B

Fire Research, 1 (1977) 57 - 66
© Elsevier Sequoia S.A., Lausanne — Printed in the Netherlands

Combustion of Wood Charcoal

D. D. EVANS* and H. W. EMMONS
Harvard University, Division of Engineering and Applied Physics, Cambridge, Mass. (U.S.A.)
(Received June 21, 1976)

SUMMARY

The dynamics of burning of wood charcoal in an air stream is examined both experimentally and theoretically. To simplify the theory, an experimental arrangement approximating a one dimensional phenomenon was adopted. The theory includes conduction in the solid, chemical reactions and heat release at the surface, and heat and mass transfer in the gas boundary layer above the surface. The molar CO/CO_2 ratio is measured. The theory predicts surface temperature, solid temperature distribution and burning rate within experimental error. An effective reaction rate formula is developed.

INTRODUCTION

This study is a step toward understanding the details of the extinguishment of wood fires by water. To avoid the complications in chemistry during the pyrolysis that wood undergoes as it burns, the initial study reported here is for the burning of wood charcoal. The burning of wood charcoal offers a simplified chemistry while maintaining a physical structure closely related to the original wood, and is an important process in a wood fire as well.

The wood charcoal used in this experiment was commercially available and produced from basswood (Tilia americana). When wood charcoal is burned, the burning surface becomes complicated by a system of cracks generated in the combustion process, and by a fiberous array of residual ash (see Fig. 1). Considering these complications, it is not surprising that little quantitative work on the combustion of wood charcoal has been done in the past. Most basic studies of carbon combustion utilize graphite which is easily obtained more chemically pure and physically uniform. Notable among the studies of graphite combustion is the extensive work performed by Nagle and Strickland-Constable [1] in which an expression for the chemical rate of reaction of pyro graphite with oxygen was developed. One might consider initially burning graphite to avoid the ash and cracking problems. However the low porosity (relative to charcoal) and the consequent large changes of properties makes such tests of little value for the present problem. In fact, graphite will not burn in the present apparatus.

The primary goal of this investigation is to predict the burning characteristics of wood charcoal from basic physical principles. Hopefully this same model will prove adequate to describe more complex cases and in particular will be helpful in the study of extinguishment. Thus it is advantageous to set up an experiment that is easily modeled. One finds that if an isolated piece of wood charcoal is ignited, it will not continue to burn unless one blows an oxidizer, *i.e.* air, on to it. A particularly useful way to blow air on it and at the same time to produce a nearly one dimensional phenomenon, is to locate the burning surface in a stagnation point flow field. In the laminar case, the stagnation point flow field develops a uniform boundary layer thickness over the impingement plane and thus uniform transport phenomenon can be expected. Unfortunately, in order to maintain combustion, air must be blown at the charcoal burning surface at high mainstream velocities; velocities that are high enough to make the flow turbulent. The degree to which the boundary layer thickness for a turbulent stagnation point flow field remains uniform, as in the

*Presently at: Center for Fire Research, National Bureau of Standards, Washington, D.C. 20234

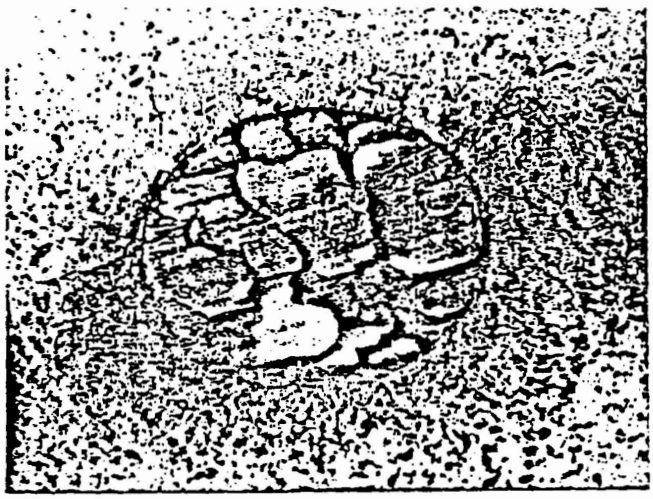

Fig. 1. Burning surface of a charcoal cylinder showing cracks and some ash cover. The circular cross-section of the surface appears elliptical because the camera was held at an angle to the axis of the cylinder to keep it out of the air flow field.

case of the laminar flow was not investigated, but the experimental results were found to be well approximated by a one dimensional theory.

The model of the burning process used here assumes that an overall reaction between carbon and oxygen takes place on the projected surface area (*i.e.* not counting the additional areas within cracks or pores; the cracks cover about 0.5% of the projected area while the pores are very small complex and constitute about 80% of the volume) to produce carbon dioxide and carbon monoxide. The energy and mass balances at the surface require a knowledge of the convective heat and mass transfer rates, the radiative heat exchange, and the conduction into the solid.

Heat transfer coefficients were measured by the cooling of a copper slug in the place of the charcoal sample. The results are presented in dimensionless form.

Mass transfer coefficients were measured by the evaporation of water from a wet porous slug in the place of the charcoal sample. The results are presented in dimensionless form and are compared with the heat transfer results.

The radiation is computed by assuming a surface emmissivity for charcoal of 0.75. This value falls within the range of literature values for "rough carbon" as for example ref. 2.

The heat conduction into the charcoal is the heat required to heat the charcoal from the ambient temperature to the surface temperature.

Finally the ratio of carbon monoxide to carbon dioxide produced during charcoal combustion was measured by a mass spectrometer analysis of grab samples. The results are compared with literature values.

BURNING RATE AND SURFACE TEMPERATURE: EXPERIMENTAL APPARATUS AND RESULTS

The wood charcoal obtained from basswood used in this experiment is that commercially sold by William Dixon Co. of Carlstadt, New Jersey, in solid blocks with

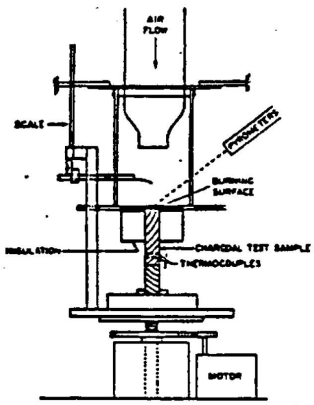

Fig. 2. Schematic diagram of apparatus.

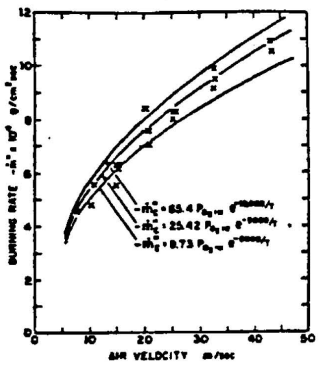

Fig. 3. Charcoal burning rate vs. mainstream air velocity; ×, experimental data; —, predicted burning rate for various kinetic parameter values.

approximate dimensions 17 × 10 × 3.5 cm.

Bulk densities ranged from 0.26 to 0.34 g/cm³ and ash content from 0.5 to 1.5% by weight. No correlation of ash concentration with the charcoal density was observed. The densities of the test charcoal fall in the same range as the densities which result from a fire, although the latter are usually riddled with cracks—large and small—while the experimental samples were free of cracks before the test and during the test only small surface cracks appeared.

To make the measurements of burning rate, surface temperature, and internal temperature distribution of a wood charcoal cylinder burning in a stagnation point flow, the apparatus schematically represented in Fig. 2 was assembled. A charcoal cylinder approximately 2.7 cm in diameter and initially 11.4 cm in height is shown burning surrounded by insulating material. This insulation is essential if the phenomenon is to be one dimensional. The charcoal cylinder is cut from a larger block of charcoal such that the grain direction is perpendicular to the axis of the cylinder. As the burning surface regresses towards the bottom of the cylinder, the motor driven platform assembly with manually operated speed control pushes the core up at the same rate as the surface is regressing. The burning surface is thus maintained at the same level as the top surface of the insulation on which the air flow impinges setting up the stagnation point flow field. Mainstream air velocities measured at the exit of the nozzle up to 45 m/sec were available. The insulation plate was held a fixed distance of two nozzle diameters from the exit of the nozzle by a larger aluminum plate with a circular opening centered on the axis of the flow.

The internal temperature distribution in the burning charcoal sample was measured by thermocouples implanted near the bottom end of the cylinder. As the burning surface regressed, the thermocouples would come closer to the burning surface eventually passing through it. From measurements of the surface positions, internal temperature information from the thermocouples could be related to their distance from the burning surface. To measure the surface position with respect to the platform, the pin on the end of a scale was lowered periodically to the surface. Contact of the pin was determined visually by observing the pin through the magnifying optics system of the pyrometer. When the pin was not in use, it was swung out of the flow field since its wake in the flow when located more than a few pin diameters above the burning surface was an unacceptably large disturbance. Aside from being used as a telescope, a disappearing filament type pyrometer was one of the pyrometers used to measure the temperature of the burning sur-

60

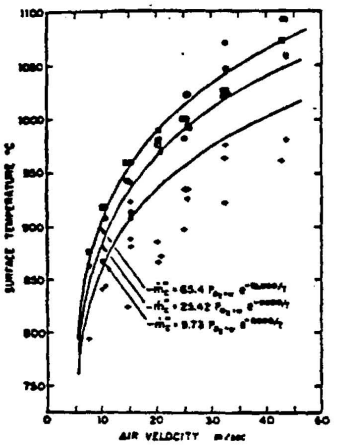

Fig. 4. Surface temperature vs. mainstream air velocity; ○, filament pyrometer; ○, infrared pyrometer; +, thermocouple; ——, predicted temperature for various kinetic parameter values.

face independent of the readings obtained from the thermocouples.

Figure 3 shows the experimental results for the steady state burning rate of the charcoal as a function of the mainstream air velocity. The burning rate of the charcoal is calculated as the product of the rate of regression of the burning surface and bulk density of the charcoal cylinder measured in room air. The carbon content of the charcoal was determined to be approximately 93% by weight. The remainder included residual hydrogen and oxygen in the charcoal structure, moisture, adsorbed gases, and ash. Thus the charcoal burning rate measured differs slightly from a carbon burning rate.

The lowest recorded mainstream air velocity at which the charcoal would self-sustain its own combustion was 7.7 m/sec. Repeated tries to burn cylinders at a mainstream velocity of 4.4 m/sec failed. After ignition on each of these trials, extinguishment began at the circumference of the burning surface near the insulation and progressed inward towards the center. This sequence of events reveals the influence of some heat loss to the insulation ring. For the purpose of analysis of these data, a self extinction velocity of 5.5 m/sec will be used.

The corresponding measurements of the burning surface temperature measured with the thermocouples and two pyrometers as a function of the mainstream air velocity are shown in Fig. 4. Pyrometer measurements are based on a surface emissivity of 0.75, which is representative of carbon surfaces at temperatures around 900 °C. The maximum temperature measured by an implanted thermocouple was generally below the measurements made by the pyrometers. This is not unexpected as near the surface it was common for the leads of the 0.025 cm diameter chromel–alumel wire threaded radially through the cylinder to be exposed by surface irregularities to the cooling effects of the air flow.

The disappearing filament type optical pyrometer manufactured by Pyrometer Instrument Company was used to measure the temperature of specific small areas of the burning surface where ash cover was a minimum. The area chosen to be measured and balancing of the instrument was left to the judgement of the operator.

The infrared pyrometer was a Barnes Engineering Co., Infrascope Mark I. This instrument was set up to give a continual reading of the average temperature in a ¼ cm² area in the center of the burning surface. Its record provided an indication of an effective surface temperature including the influence of the ash layer. Because of fluxuations caused by pieces of ash cover being swept away in the air flow and changing surface crack patterns, some judgement was exercised in assigning one value of temperature characterizing the output. Generally the uncertainity associated with these measurements is ±15 °C.

Close examination of the pyrometer data reveals that the measurements made with the infrared pyrometer, influenced by the ash layer, are approximately 25 °C lower than those made with the filament pyrometer, measuring temperatures in areas of minimum ash concentration, for low air velocities. With increasing air velocity, the two sets of data blend together. This trend indicates the decreasing influence of the ash layer at higher air velocities, as it is swept from the surface more easily than at lower velocities. At the highest air velocity, 43 m/sec, the measurements with the infrared pyrometer are re-

corded as higher than those with the filament pyrometer. This could indicate that the chosen emissivity for the burning surface is too low. Assuming that the influence of the ash is negligible at this high air velocity, the value of the surface emissivity that brings both pyrometer measurements into agreement at 43 m/sec and 1055 °C is 0.85. It is also likely that the differences in temperature recorded are simply the result of uncertainties in the measurements as they approach the limits of accuracy for the measurements.

BURNING RATE AND SURFACE TEMPERATURE: THEORETICAL MODEL

As mentioned in the introduction, a one dimensional model is adequate for these experimental results. It is desirable to know the detailed chemical kinetic mechanism involving reactions at the carbon surface, in cracks and pores, and in the gas phase. Unfortunately sufficiently detailed chemical data was not found. The graphite reaction kinetic formula of Nagle and Strickland-Constable [1] was tried but as expected was wholly inadequate (low by a factor of about 50). A measurement of the local density near the charcoal surface suggests some burning in the pores and cracks (up to 10%). With charcoal there is no significant burning out in the boundary layer or else the fire could be "blown out" as is the case with burning polymethylmethacrylate. The absence of such major boundary layer burning does not preclude minor reactions in the boundary layer nor major reactions in the gas phase very close to the charcoal surface.

In the absence of applicable chemical data, we will assume an overall reaction and reaction kinetics formula applicable to the charcoal projected surface area. Thus we assume an effective surface reaction:

$$C + xO_2 \rightarrow aCO + bCO_2 \qquad (1)$$

where

$$a + b = 1 \qquad (2)$$

$$x = \frac{a}{2} + b \qquad (3)$$

As discussed later the CO to CO_2 molar ratio is given by

$$a/b = 4.3 \exp(-3390/T) \qquad (4)$$

and the reaction rate is assumed in the form of a first order Arrhenius reaction.

$$-\dot{m}_C'' = A p_{O_2,w} \exp(-E/RT) = K p_{O_2,w} \qquad (5)$$

Prediction of the burning rate and surface temperature of the charcoal in steady state combustion is done by solving simultaneously two independent equations relating the burning rate and surface temperature. The first equation involves an energy balance at the burning surface equating the energy generated in the above chemical reaction to that lost through heat transfer. The burning rate of the charcoal based on the surface energy balance is given by:

$$-\dot{m}_C'' = [h(T_w - T_a) + \epsilon\sigma(T_w^4 - T_s^4)] / \left[-a\Delta H_{CO}^\circ - b\Delta H_{CO_2}^\circ + \left(c_C + x\frac{M_{O_2}}{M_C}c_{O_2} - a\frac{M_{CO}}{M_C}c_{CO} - b\frac{M_{CO_2}}{M_C}c_{CO_2}\right) \times (T_w - T^\circ) - c_C(T_w - T_a)\right] \qquad (6)$$

In eqn. (6), the value of h is given as shown later by:

$$Nu = hd/k = 3.5\,(RePr)^{0.25} \qquad (7)$$

The second equation relating the burning rate and surface temperature is eqn. (5) which however requires the oxygen partial pressure at the burning surface. The oxygen partial pressure at the surface $p_{O_2,w}$ is determined from the conservation of species equations at the burning surface. For oxygen this takes the form:

$$h_m(Y_{O_2,a} - Y_{O_2,w}) + \dot{m}_C'' Y_{O_2,w} = -\dot{m}_C'' \frac{M_{O_2}}{M_C} x \qquad (8)$$

Similar balances for all the other species are needed to determine the composition of the mixture of gases at the burning surface in order to find the oxygen partial pressure. For this calculation the transport rate per unit concentration difference of each species is considered equal to that for oxygen. As described later, the mass transfer coefficient is given by

$$Sh = h_m d/\rho_{air} D = 2.7\,(ReSc)^{0.4} \qquad (9)$$

The oxygen partial pressure at the surface is thus found to be

$$p_{O_2,w} = p\left[1 + \frac{\frac{M_{O_2}}{M_{N_2}} h_m Y_{N_2,a} - \frac{M_{O_2}}{M_C}\dot{m}''_C b - \frac{M_{O_2}}{M_C}\dot{m}''_C a}{\dot{m}''_C x \frac{M_{O_2}}{M_C} + h_m Y_{O_2,a}}\right]^{-1} \quad (10)$$

Substitution of this expression into eqn. (5) yields the second equation relating the burning rate and the surface temperature after some manipulation as:

$$-\dot{m}''_C = \frac{M_C}{M_{O_2}(x-1)}\left[\left(Kx\frac{M_{O_2}}{M_C}p + h_m Y_{O_2,a} + \frac{M_{O_2}}{M_{N_2}}h_m Y_{N_2,a}\right) - \left\{\left(Kx\frac{M_{O_2}}{M_C}p + h_m Y_{O_2,a} + \frac{M_{O_2}}{M_{N_2}}h_m Y_{N_2,a}\right)^2 - 4h_m Y_{O_2,a} K\frac{M_{O_2}}{M_C}(x-1)p\right\}^{1/2}\right] \quad (11)$$

Solutions for the steady burning rate and surface temperature satisfying eqns. (6) and (11) were found as a function of the mainstream air velocity and values for all the parameters in the reaction rate expression eqn. (5). In all the predictions, a pressure of 1 atm and an ambient temperature of 20.4 °C representing the average value during all the tests yielding the data recorded in Figs. 3 and 4 was used.

The most powerful piece of information obtained from the data in terms of predicting values of the rate parameters A and E/R was the determination of the self-extinction velocity. From experiments, the minimum air velocity at which the charcoal will sustain its own combustion can only be said to be between 4.4 and 7.7 m/sec. For determining appropriate values of the parameters A and E/R, assumed to be constant, the value of the air velocity set as the self-extinction velocity was 5.5 m/sec. Choosing a value for E/R, a corresponding value for A can be found such that no solution to eqns. (6) and (11) representing steady burning exists at air velocities below 5.5 m/sec. Following this procedure, the lines on Figs. 3 and 4 show the calculated results for burning rate and surface temperature for three values of E/R—8000, 9000 and 10,000—assuming an emissivity for the burning surface of 0.75. The corresponding value of A is given in each case. Comparing the calculation to the experimental data, one can see that in all cases the general agreement is good. The combination of E/R = 9000 (°K) and A = 25.42 (g/cm² sec atm) results in the best agreement considering both sets of experimental data.

Because the extinction velocity is important in the determination of the constants A and E/R, some analysis was performed to determine the effect of the uncertainty in this value on the results. Varying the extinction velocity above and below 5.5 m/sec by 1.5 m/sec for a value of E/R equal to 9000, changed the value of A to 24.19 and 27.31 respectively. In terms of an overall first order reaction occurring on the surface, the form of the expression for the effective chemical kinetic rate of reaction applicable to wood charcoal oxidized in air is:

$$-\dot{m}''_C = (25.4)p_{O_2,w}e^{-(9000/T)} \ (\mathrm{g\ cm^{-2}\ s^{-1}}) \quad (12)$$

The value of E/R of 9000 found applicable to wood charcoal compares favorably with a value of 8160 found useful for Austrian brown coal char in a work by Hamor, Smith and Tyler [3]. Both of these values do not agree well with the 15,100 value of E/R found applicable to the oxidization of pyro graphite in the work of Nagle and Strickland-Constable [1]. A possible explanation for the difference between the results for graphite and those for coal char and charcoal could be the influence of a substantial amount of burning occurring in pores opening onto the surface. Under certain conditions, combustion in pores as opposed to that on an exposed surface can lower the observed activation energy by a factor of two from the actual value associated

with the reaction occurring at the burning surface. A detailed discussion of this effect is given by Wheeler [4].

THE TEMPERATURE DISTRIBUTION WITHIN THE UNBURNED SOLID

To model the temperature distribution in the charcoal below the burning surface, a steady state solution to the one-dimensional heat conduction equation in a semi-infinite solid was sought. The burning surface was assumed to have constant temperature T_w and to travel at a constant velocity V, (with respect to a coordinate system fixed to the base of the charcoal cylinder) into the unburned solid, initially at uniform temperature T_0.

No steady state solution exists in a frame of reference in which the surface moves; but with respect to a system in which the burning surface remains fixed in space, the steady state solution is:

$$(T - T_0) = (T_w - T_0)\exp(-VX/\alpha) \qquad (13)$$

To obtain eqn. (13) all the properties of the charcoal forming the thermal diffusivity α, ($\alpha = k/\rho c$), were assumed constant, and heat flux only in the axial direction was allowed.

The exponential form of the anticipated temperature profile suggests that a useful way to plot the experimental results would be in the form of $\ln(T - T_0)$ *vs.* X. From eqn. (13) it would be expected that a straight-line with slope $-V/\alpha$ would result.

Figure 5 shows the experimental results for a charcoal cylinder with density 0.329 g/cm^3 and initial temperature of 19.7 °C burned in mainstream air velocity of 21 m/sec. The temperature outputs from two thermocouples located on the axis of the cylinder and initially 99.2 mm and 104.3 mm from the end of the cylinder to be burned, (1 and 2 respectively in Fig. 2), are shown as functions of the distance from the burning surface. The plot yields a rough straight-line with mark deviations at large distances from the burning surface and in the range of temperature difference equal to 100 °C. At large distances from the burning surface, the deviation is caused by termination of the insulation around the cylinder at 56 cm. The deviation in the region of a temperature difference of 100 °C is believed due to

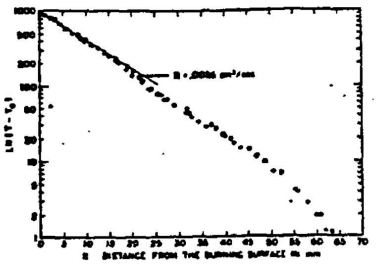

Fig. 5. Experimental data for the steady state internal temperature distribution in a charcoal cylinder with density 0.329 g/cm^3, and initial temperature (T_0) of 19.7 °C burned in a mainstream air velocity of 21 m/sec. Data shown from the thermocouples (+) and (O) initially 99.2 mm and 104.3 mm from the burning surface respectively. Line: straight line fit of data near burning surface.

desorption of adsorbed gases from the charcoal structure.

From a knowledge of the surface velocity, V, (for this test 0.138 cm/min) and the slope of the data near the burning surface, a value of the thermal diffusivity of wood charcoal appropriate to that temperature range can be found as indicated by the results of the simple conduction model. The straight-line fit of the data shown in Fig. 5, yields a value for the thermal diffusivity, α, of 0.0026 cm^2/s. Use of the slope of the data at lower temperatures to predict the thermal diffusivity using the result of the simple conduction model, eqn. (13) would be inappropriate because of the influence of the desorption region, the termination of the insulation, and consequent radial heat loss.

A modest attempt was made to calculate the thermal diffusivity from measurements of the basic properties of thermal conductivity, density and specific heat. The thermal conductivity of wood charcoal was measured and is given by

$$k = 0.0016\rho - 0.00017 \text{ (cal cm}^{-1}\text{ s}^{-1}\text{ °C}^{-1}) \qquad (14)$$

applicable at room temperature, and the specific heat was measured at room temperature and was found to be 0.24 (cal g^{-1} °C^{-1}).

The resultant thermal diffusivity was 0.0045 cm^2/sec to be compared with 0.0026 cm^2/sec found from the burning experiment.

The exact reason for the discrepancy was not sought but is probably associated with the fact that the burning test value is in a higher temperature range where the adsorbed gases have been expelled from the charcoal.

HEAT AND MASS TRANSFER COEFFICIENTS

To measure the convective heat transfer rate as a function of the mainstream air velocity, a copper cylinder the same diameter as the charcoal cylinders being used was set into the insulation so that it occupied the same position the charcoal would normally. The rate of energy lost as it cooled from 350 to 250 °C was determined. This measurement was corrected for heat lost to the insulation to find the convective heat loss rate from the exposed surface. The mass transfer characteristics of the flow field were determined from measurements of the rate of evaporation of water from a sintered disk of the same diameter and located in the same position in the air flow as a charcoal cylinder.

The non-dimensionalized results of the experiment are shown in Figure 6. The results for the heat and mass transfer rates are fit by eqns. (7) and (9) respectively. All of the properties used in the non-dimensionalization are evaluated at the film temperature, the average between the surface and ambient temperatures. The binary diffusion coefficient for water into air, D_{H_2O-air}, was calculated from an expression developed from kinetic theory by Chapman and Enskog [5]. Good agreement among the two sets of measurements in terms of the analogy between convective heat transfer and mass transfer rates is revealed.

Also shown in Fig. 6 are the results for heat transfer in a turbulent stagnation point flow taken from Garden and Cobonpue [6] and Jakob [7]. In selecting results from these sources an effort was made to preserve the ratios of the distance of the stagnation plane from the nozzle exit to the nozzle diameter (l/d) and diameter of the nozzle to the diameter of the circular heat transfer surface (d/s).

CARBON MONOXIDE FORMATION DURING BURNING

To determine the energy released in the combustion of the charcoal, it is necessary to

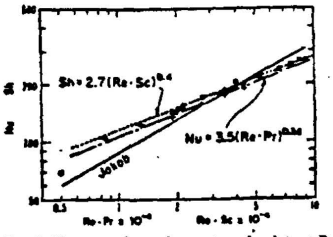

Fig. 6. Heat transfer and mass transfer data. + Present heat transfer measurement, $l/d = 2$, $d/s = 1.94$. □ Present mass transfer measurement $l/d = 2$, $d/s = 1.94$. ● Data from Garden and Cobonpue [5] ($Pr = 0.72$) $l/d = 2$, $d/s = 2.51$. — · — $Nu = 3.5(RePr)^{0.36}$; least squares fit of +; - - - - - $Sh = 2.7(ReSc)^{0.4}$; least squares fit of □; ——— $Nu = 0.533(ReFr)^{0.573}$; from Jakob [6] ($Pr = 72$); $l/d = 1.43$, $d/s = 1.75$.

determine the ratio of carbon monoxide to carbon dioxide formed in the reaction. Samples of gas extracted from a region just above the level of the surface and at the circumference of the burning surface, were analyzed for the CO/CO_2 ratio with a mass spectrometer. Figure 7 shows the results plotted as a function of the surface temperature. Originally the data were collected as a function of the mainstream air velocity of the flow indicated at the top of Fig. 7. Characteristic surface temperatures as a function of the air velocity shown in Fig. 4 from the infrared pyrometer were used to convert the data from an air velocity dependence to surface temperature dependence.

Also indicated in Fig. 7 is the result of Arthur [8] for the CO/CO_2 ratio produced in the combustion of graphite and coal char granules in a quartz reacting vessel. The relation $X_{CO}/X_{CO_2} = 10^{3.4} \exp(-12{,}400/T)$ he determined from analysis of the products of the carbon reaction with a flow of oxygen nitrogen, and a small amount of phosphoryl chloride ($POCl_3$) vapor. The $POCl_3$ was added to inhibit the gas phase reaction of carbon monoxide to carbon dioxide. In a previous study [9], the effect of this inhibitor on the ratio of carbon monoxide to carbon dioxide formed during the oxidation of graphite was examined. It was found that a concentration of $POCl_3$ of less than 1% in the air flow raised the CO/CO_2 ratio in the products of combustion to 8.4 from a value of 0.05 (shown in

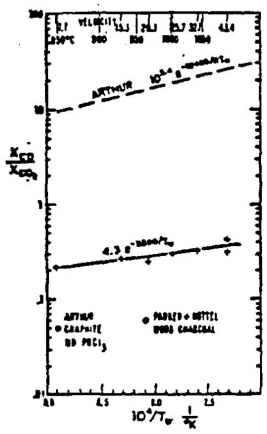

Fig. 7. Molar ratio of CO/CO_2 vs. inverse surface temperature.

Fig. 7 with no inhibitor present). Also shown in Fig. 7 is one value for the CO/CO_2 ratio measured in the combustion of charcoal by Parker and Hottel [10]. Comparing the results of the measurements reported here to those of Arthur would suggest that some gas phase reaction is involved in our combustion of wood charcoal. Because of the high air velocities used in this experiment, if a gas phase reaction does exist it must be confined to a region very close to the burning surface.

CONCLUSIONS

The simple surface combustion model presented in this work can be used to predict the burning rate and surface temperature of wood charcoal burned in a stagnation point flow of air.

An expression for the effective chemical rate of reaction of wood charcoal oxidized in air has been developed. Since this result is empirical and not based upon detailed chemical mechanisms, further work is required to determine the extent of its applicability.

Predictions of the internal temperature distribution in the burning sample can be made based on a simple one-dimensional conduction model in a semi-infinite solid, if a value for the thermal diffusivity appropriate to wood charcoal at elevated temperatures can be obtained and adequate insulation is used around the burning sample.

Results of this study imply that both a gas phase reaction and substantial combustion in pores may be involved in the oxidation of wood charcoal in air. These detailed mechanisms still need elucidation.

ACKNOWLEDGEMENTS

This work is a result of the thesis study of Evans and was supported in part by the National Science Foundation under Grant NSF GI34734, and by the Division of Engineering and Applied Physics, Harvard University.

LIST OF SYMBOLS

a	Moles of CO produced per mole C burned
A	pre-exponential factor, g/cm² sec atm
b	moles of CO_2 produced per mole C burned
c	specific heat, cal/g °C
d	diameter of the air nozzle
D	binary diffusion coefficient, specie i into air, assumed all equal to oxygen in calculation, cm²/sec
E	activation energy, cal/g-mole
h	heat transfer coefficient, cal/cm² sec K
ΔH_i	negative of the heat of combustion of charcoal to product i, cal/g carbon
h_m	mass transfer coefficient, g/cm² sec
k	thermal conductivity, cal/cm sec °C
K	$A \exp(-E/RT)$
l	distance from nozzle exit to impingement plane, cm
$\dot{m}''$	rate of increase of mass per unit time per unit area, g/cm² sec
M	molecular weight
Nu	Nusselt number, hd/k
p	pressure, atm
p_i	partial pressure of specie i, atm
R	ideal gas constant, cal/g-mole °K
RePr	product of Reynolds and Prandtl numbers, vd/α
ReSc	product of Reynolds and Schmidt numbers, vd/D

s	diameter of heat flux sensor, cm
Sh	Sherwood number, $h_m d/\rho_{air} D$
v	mainstream air velocity, cm/sec
V	surface velocity, cm/sec
x	$(a/2) + b$ [see eqns. (1), (2), (3)]
X	distance from the burning surface into the solid, cm
X_i	mole fraction of species i
Y_i	mass fraction of species i

Greek

α	thermal diffusivity, $k/\rho c$, cm^2/sec
ϵ	surface emissivity
ρ	density, g/cm^3
σ	Stefan-Boltzmann constant, cal/cm^2 sec K^4

Subscripts

a	ambient
air	air
C	carbon
CO	carbon monoxide
CO_2	carbon dioxide
m	property of the mixture
N_2	nitrogen
O_2	oxygen
w	burning surface
0	initial value

Superscript

*	at the reference temperature for the heats of formation—18 °C

REFERENCES

1 J. Nagle and R. F. Strickland-Constable, Oxidation of carbon between 1000 and 2000 °C, Proc. Fifth Carbon Conf., 1 (1961) 154 - 164.
2 G. G. Guboreff, J. E. Jaussen and R. H. Torborg, Thermal Radiation Properties Survey, Honeywell Research Center, Minneapolis, Minn., 2nd edn. (1960).
3 R. J. Hamor, I. W. Smith and R. J. Tyler, Kinetics of combustion of pulverized brown coal char between 630 and 2200 K, Combustion and Flame, 21 (1973) 153 - 162.
4 A. Wheeler, Reaction rates and selectivity in catalyst pores, Adv. Catalysis and Related Subjects, Vol. 3, Academic Press, New York, 1951, pp. 275 - 282.
5 R. Bird, W. Steward and E. Lightfoot, Transport Phenomena, Wiley, New York, 1960, pp. 510 - 512.
6 R. Gardon and J. Cobonpue, Heat transfer between a flat plate and jets of air impinging on it, Intern. Heat Transfer Conf., University of Colorado, 1961.
7 M. Jakob, Some investigations in the field of heat transfer, Proc. Phys. Soc. London, 59 (1947) 726 - 755.
8 J. R. Arthur, Reactions between carbon and oxygen, Trans. Faraday Soc., 47 (1951) 164 - 178.
9 J. R. Arthur, D. H. Bangham and J. R. Bowring, Kinetic aspects of the combustion of solid fuels, Third Symp. on Combustion, Flame, and Explosion Phenomena, Williams and Wilkins Co., Baltimore, Maryland, 1949, pp. 466 - 474.
10 A. S. Parker and H. C. Hottel, Combustion rate of carbon study of gas-film structure by microsampling, Ind. Eng. Chem., 28 (1936) 1334 - 1341.

Nuclear Consulting Services, Inc.
PO BOX 29151 COLUMBUS, OHIO 43229

Attachment II to
Hazards Analyses of
Seabrook Station
Charcoal Filter Units,
YAEC 1571

Iodine Adsorber Fire Test

performed for

Yankee Atomic Electric Co.
New Hampshire Yankee

under PO No. 46114

15 Sept 1986

DISTRIBUTION

YAEC: D.M. Pepe (3) + (1) by Telefax

PLC: M.E. Mowrer (1) by Fed. Exp.

NUCON: P.G. Lafyatis
M.N. Magnus
J.M. Stephens
W.P. Freeman
J.L. Kovach
08PS942 MF

08PS942/01

Introduction

The impregnated carbon used in the various air cleaning systems is typically protected from fire by water deluge systems. The initiation of the water deluge normally takes place by temperature rise signal. This type of fire control has several inherent problems:

a) temperature rise will indicate only major, fully developed fire

b) water distribution in pleated carbon beds is non uniform

c) very large amounts of potentially contaminated water are generated.

To avoid these problems a system test was performed to evaluate the detection of carbon oxidation by CO monitoring and to throttle carbon fires by stopping forced airflow through the carbon bed. Tests were perfromed in both the ASTM ignition test rig and in the Fire Wind Tunnel (FWT) to evaluate CO penetration and temperature generation.

Description of the Equipment & Procedures

1) The ASTM D3466 Test Rig which consists of heated air flow through a carbon bed with inlet air, inlet carbon bed and outlet carbon bed temperature measurement. The test is normally performed at 100 FPM velocity, however, for these tests the airflow was reduced to 40 FPM which is the design velocity of the Seabrook air cleaning systems. The bed depth normally is 1.0 inch deep for these tests. Two inch deep beds of 50 ml (~25g) of carbon was used.

2) The NUCON fire wind tunnel (FWT) consists of an adjustable flow blower followed by an indirect fired natural gas furnace to heat the air, and an adjustable plenum to hold a 24 inch X 24 inch face area adsorber specimen, and the commensurate reduction for outlet ducting.

For these tests a 4.0 inch deep carbon bed was used filled with 2% KI and 2% TEDA impregnated carbon. The inlet temperature to the carbon bed was monitored at a single point in the center area four inches from inlet face of the adsorber. The outlet face of the adsorber was instrumented at 4.0 inches away from the adsorber with five thermocouples. The CO monitor (an infrared sensor type) was taking samples 2 feet down stream from the filter outlet face in the 10 inch reduced duct section.

The adsorber	full weight before fire was	65.8 lbs
	empty weight	18.4 lbs
	as is carbon weight	47.4 lbs
	dry carbon weight (less H_2O)	43.6 lbs

When the test was performed, the gas heater was turned on maximum heat to accomplish as fast heat-up as possible. Air flow was maintained for five minutes after fire was detected, then airflow was stopped and the carbon bed inlet and outlet temperatures monitored for 1 hour. The carbon bed was removed from the FWT and weighed.

Test Results

The test (result of the carbon burning test) in the ASTM rig was conducted until all of the carbon was consumed at 40 FPM velocity. The temperatures of the inlet and outlet carbon bed are shown on Table 1.

The results of the fire wind tunnel (FWT) test are shown on Table 2 and on Figure No. 1.

The pertinent values are as follows:

CO of 50 ppm at 11 minutes
CO off scale (200+ ppm) at 19 minutes
Fire in carbon bed at 19:15 - 19:45 minutes
Airflow stopped at 24 minutes

Maximum Temperature 4.0 inches from outlet face	375°C
Temperature at 1.0 hour after ignition with no air flow 4.0 inches from outlet face	200°C
Carbon loss, total test duration (excluding moisture and 2% TEDA which would evaporate in test)	4.53 lbs
Carbon monoxide signal sharply increasing at inlet temperature of	175°C
Filter frame (304 SS) bright red at	24 minutes

Evaluation of the Test Results

The configuration of air cleaning systems is such that the iodine adsorbers are preceded by HEPA filters. The HEPA filter mounting frame is a steel structure with 22 inch X 22 inch openings, therefore, no larger burning material than one HEPA filter size could enter from the carbon bed, anything larger would be stopped by the HEPA mounting frame structure even if it would penetrate the preceding components. This was the reason for the selection of a 24 inch X 24 inch carbon section for the FWT test.

The Seabrook procedure is based on shut down of the airflow 5 minutes after a CO alarm. However, to maintain conservatism in the test, the airflow was shut down NOT 5 minutes after CO alarm, but 5 minutes after actual burning of the carbon in the test section. Even under these conditions the maximum temperature at 4.0 inches from the outlet face of the adsorber was only 375°C, and the temperature started to drop as soon as the blower was shut off. It is important to note that no isolation dampers were closed in the inlet and outlet of the FWT, thus natural air convection was maintained during the test even with the blower shut off, which is another conservatism because most air cleaning systems are equipped with outlet dampers and several are isolatable on both inlet and outlet side.

The ASTM test rig data indicates (from Table 1) that even with airflow maintained, approximately one hour is needed to burn 2.0 inch depth of carbon. While the results from the FWT test indicate that if airflow is stopped five minutes after carbon burning only approximately 10% of the carbon is burned in one hour. While if the carbon monoxide signal is used for system isolation, the fire itself will probably be prevented.

The sharp increase in CO concentration at 175°C inlet air temperature was also determined in the ASTM test rig at 40 FPM and it indicated sharp rise at 175°C inlet air temperature while autoignition did not take place until in excess of 250°C inlet air temperature.

Conclusions and Recommendations

Carbon monoxide monitoring is a very good detection method of carbon oxidation PRIOR TO ACTUAL selfsustained burning of the carbon. Isolation of the system indicating fire within five minutes of CO signal will probably prevent development of selfsustaining carbon fire. Isolation of the system can, after the fire develops during air flow, result in sharp temperature drop upon isolation of the air flow. The maximum temperature 4 inches downstream of the burning carbon bed with air flow at 40 FPM was 375°C.

Based on these results it is recommended that CO monitors be installed in the housing at outlet of the housing and another preferably in the inlet area (just upstream from carbon beds at the top of housing, since CO is lighter than air)

The system should be isolated within five minutes of a CO signal of 50 ppm maximum.

Table 1

08PS942

Test Date
3 Sept 1986

Carbon ignition followed by residual heating (i.e. air flow continued but heat off).

Method: ASTM D3466 except: 40 FPM, 2 inch bed depth and fast heat up

Material: Dry air and NUSORB KITEG II Lot 45/10

Starting condition: 25°C

Ignition occurred at an upper bed (outlet) temperature of approximately 400°C, lower bed (inlet) temperature of 285°C, air inlet temp. 285°C.

Temperatures after ignition:

	Within Carbon Bed	
Time (Min.)	Outlet Side (°C)	Inlet Side (°C)
0:15	790	255
1:00	700	920
2:00	650	850
3:00	640	800
4:00	730	800
5:00	760	805
6:00	790	790
7:00	835	780
8:00	860	790
9:00	920	790
10:00	950	780
11:00	980	730
12:00	1050	800 purple smoke
15:00	780	450
20:00	375	250
30:00	210	150
60:00	100	135

08PS942/01

Table 2

FWT Test Data

Time (Min.)	CO Level (ppm)	Inlet Temp (°C)	Maximum of five (5) Outlet Temps. (°C)
0	2	28	28
4	5	75	35
7	10	125	35
10	20	---	40
11	28	150	---
12	38	---	40
13	44	---	40
14	60	160	---
15	78	---	45
16	102	---	45
17	146	170	---
18	172	---	50
19	Off Scale		50
	Smoke coming out of test rig exhaust		
20		175	200
23		250	375
24	Shut down fan and furnace		
	Filter frame top glowing red		
26		375	320
28		350	---
30		---	260
33		320	250
35		300	---
36		300	---
38		280	---
40		275	225
44		260	225
47		250	220
75		205	195

Both inlet and outlet temperatures at 4.0 inches from filter face in the flow direction.

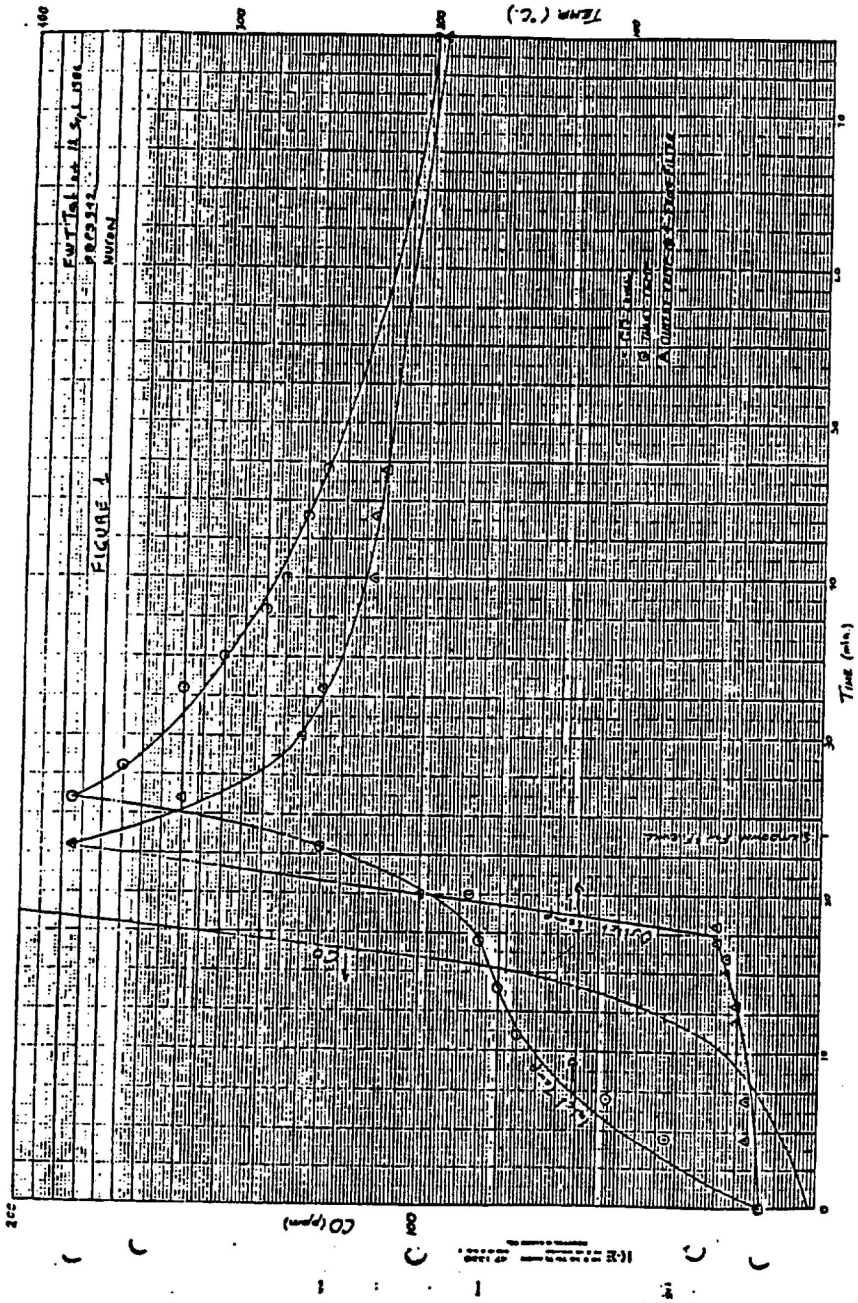
FIGURE 1
TEMP (°C)
CO (ppm)
TIME (min)